Radar & Additive Manufacturing Technologies: the Future of Internet of Things (IoT)

Jimmy G.D. Hester, John Kimionis, Ryan Bahr, Wenjing Su, Bijan Tehrani, and Manos M. Tentzeris
School of Electrical and Computer Engineering, Georgia Institute of Technology,
Atlanta, GA, 30332 USA e-mail: jimmy.hester@gatech.edu

***Abstract*—The authors make a case for a soon-to-be preponderance of radar technologies for communications with devices of the IoT. First, the tag architectures enabling these communications are presented. Novel $24\,\mathrm{GHz}$ and mm-wave flexible low-cost chipless RFID and backscatter/reflectarray-based node approaches demonstrating a record measured range of $80\,\mathrm{m}$, with a potential maximum range in excess of $1\,\mathrm{km}$, zero to low $\mu\mathrm{W}$ power consumption, and Gbps communications rates are presented. In a second part, recent advances in additive-manufacturing technologies—enabling large cost reductions for the next generation of integrated radar ICs—are reported. Specifically, the combination of 3D and inkjet printing enables the development of fully 3D compact low-cost integrated modules along with high-performance interconnects. These innovations, simultaneously empowering and empowered by radar technologies, present a compelling avenue for the emergence of dense constellations of flexible smart skin nodes for ubiquitous sensing, identification, and localization.**

***Index Terms*—Remote sensing, mm-wave, Chipless RFID, Inkjet printing, Flexible electronics, Internet of Things, Smart Skin**

I. Introduction

The Internet of Things (IoT) promises to enable all object, items, and surfaces with wireless identification, sensing, and actuation capabilities, thereby meshing large agricultural, industrial, urban, and infrastructural environments into clusters of wirelessly-connected nodes. While economically and technologically enticing of a concept, current hardware limitations are preventing the growth of the IoT past a limited set of specific contexts. Two of the greatest challenges are those of power and compactness/inconspicuousness, and their trade-off space relative to other essential specifications such as communication range and ability to be placed onto metallic surfaces. One can largely categorize current IoT nodes into two groups: active transmitters and RFIDs. The former require the generation of an RF signal (typically in the $900\,\mathrm{MHz}$ or $2.4\,\mathrm{GHz}$ bands) by the node, which can only be achieved at the cost of a minimum of about $10\,\mathrm{mW}$ of instant power consumption. The later, by contrast, relies on backscatter schemes which can enable communications using instant powers as low as $500\,\mathrm{nW}$. Despite their higher power consumption, active devices are dominant in most application contexts due to their maximum reading range ($0.4\,\mathrm{km}$ to $40\,\mathrm{km}$ depending on what technology is considered) which greatly surpass that of passive ($10\,\mathrm{m}$) and semi-passive ($25\,\mathrm{m}$) RFIDs. The reasons underlying these range limitations stem from wireless power transfer limitations (due to regulations) and limited tag receiver sensitivities, for passive and semi-passive RFIDs, respectively. The presence of these receivers is generally deemed necessary in order to structure communications between the readers and the multiple tags as well as to collisions between messages that could be concurrently received by the reader. In addition to these considerations, the current operation frequencies of these aforementioned IoT devices preclude their implementation onto thin flexible and conformable substrates without incurring substantial antenna-performance degradation induced by the proximity of their mounting surface; this effect becomes all the more severe upon mounting onto metal surfaces. In this paper, the authors make the case that radar technologies, used in tandem with low-cost, thin, and flexible $24\,\mathrm{GHz}$ and mm-wave RFID reflectarray targets, will provide a cost-effective and extremely capable alternative to current hardware solutions for the IoT. First, the approach is introduced, the two types of tag topologies (chipless and not) are outlined and their specifications discussed before practical demonstrations of their implementation for two applications—long-range sensing and Gbps data transfer—are shown and commented upon. Secondly, recent technological advances in additively-manufactured packaging for the performance-enhancement and cost-reduction of mm-wave modules are reported, thereby demonstrating a strong foundation for the commercial emergence of ultra-low-cost fully-integrated radar reading systems. Finally, a conclusion is drawn.

II. RFID targets for radar readers

A. General system perspective

The reader/tag systems considered in this paper consist of readers with radar capabilities that generate a signal that impinges onto active or passive tag targets. These tags can display several architectures, from which two main categories can be distinguished: chipless and not.

1) Chipless targets: Chipless targets are a staple of the field of "Chipless RFIDs", and are designed to scatter the impinging signal while enabling this response with distinctive and detectable properties, thereby encoding information. Data can be engineered as resonances (magnitude minima) in the response frequency spectrum, with the presence or absence of a set of N resonant frequencies encoding an N-bit binary number. The analog magnitude of the response is also used to translate data, although it is much more challenging to accurately measure. The main challenge of this approach is that of isolating the response of the tag from that of the environmental clutter and the self-interference of the reader itself. Because of this difficulty, chipless targets have traditionally been limited

978-1-5386-4167-5/18/$31.00 ©2018 IEEE

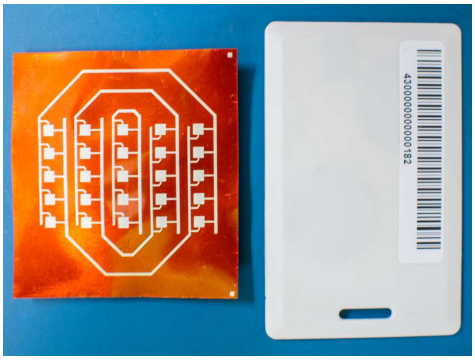

Fig. 1. Fully-inkjet-printed Van-Atta reflectarray [1]

to ranges of less than about $3\,\mathrm{m}$. This was achieved by using Ultra WideBand (UWB) [2] tags whose response could be extracted using time-delay discrimination and, therefore, ranging. Very recently, another method using radar principles has increased the reading range of the state-of-the-art chipless RFIDs to $58\,\mathrm{m}$. This work, reported in [1], [3], relied on the combination of a high-performance tag/signal-processing approach. The proof-of-concept tag prototype, shown in Fig. 1, is a Ka-band fully-inkjet-printed flexible Van-Atta reflectarray whose response is cross-polarized relative to the signal impinging on it from the reader, thus resulting in a drastical increase of the signal-to-clutter-interference-ratio measured during interrogation, leading to an unprecedented interrogation range in excess of $30\,\mathrm{m}$ in a cluttered indoor environment. This was enabled by the extraction of the tag-response signal using a novel (in this field) matched-window spectrogram approach, whose output is shown on Fig. 2.

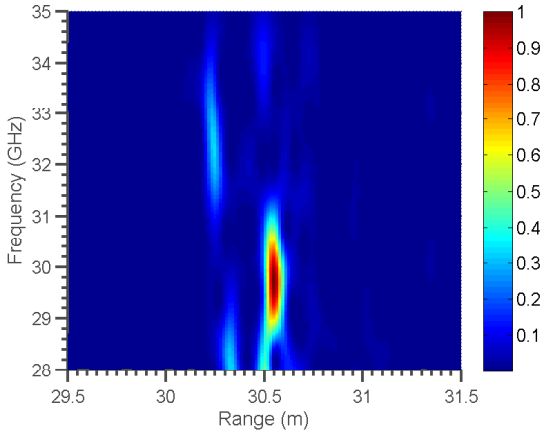

Fig. 2. Spectrogram of tag (shown in Fig. 1) detection around $30\,\mathrm{m}$ [1]

For the first time, this method also allowed for the identification and discrimination of multiple targets in the two dimensions of time-delay and resonant frequency, as displayed in the spectrogram shown in Fig. 3. A similar target was also interrogated using a scanning FMCW radar, thereby extending its demonstrated range to $58\,\mathrm{m}$ [4].

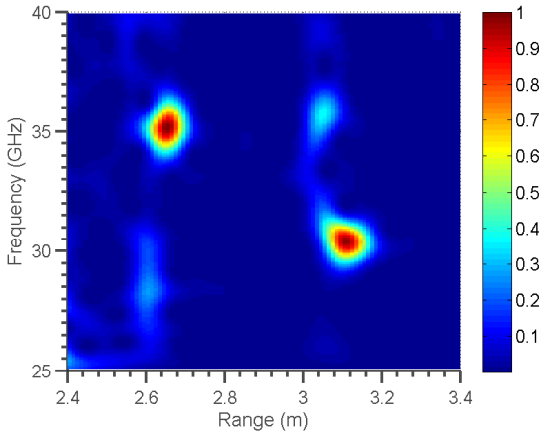

Fig. 3. Spectrogram of the concurrent detection of two chipless tags [1]

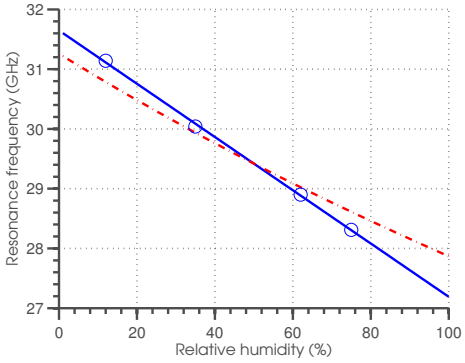

Fig. 4. Measured (blue full) and modeled (red dashed) shifts in the resonant frequency of the tag of Fig. 1 as a function of the ambient relative humidity level [1]

2) Ultra-low-power targets: While the performance of chipless tags has witnessed tremendous progress in the last decade, their reading range and features remain quite limited. This is mostly the consequence of the linearity of the tag, whose information cannot therefore be sufficiently distinguished spectrally from the interference. This consideration results in a very direct solution: introduce non-linearities in the tag in order for the backscattered signal to hold a richer set of frequency components. This can be achieved through the introduction of an unbiased diode-based frequency doubler in the tag, as has been done for "Harmonic radars" [5]. This solution allows for the spectral discrimination without the inclusion of a power source. However, because of the input-power-dependent efficiency of the doubler, these approaches suffer losses according to a R^{-6} (where R is the reading range) and are not empowered by the wealth of features offered by low-power active electronics components, due to their lack of power supply. An alternative strategy is to apply backscatter modulation, where the Radar Cross Section (RCS) of the target is dynamically modulated through the use of nW switches. This latter strategy, used by typical RFIDs ($900\,\mathrm{MHz}$ or lower), has the advantage of conserving the R^{-4} loss law

while simultaneously enabling the use of widely-capable active electronics. Nevertheless, the need to avoid collisions between the signals received from a non-synchronized constellation of nodes has necessitated the integration of range-limiting receivers in current tags. The rise of backscatter RFIDs to the K-band and above is now promising to enable a quantum leap in reading ranges and data transmission rates through the combined effect of better link budgets [1] (for given tag and reader sizes) as well as the ability to discriminate between receiver-less tags through high-resolution angular and range localization (i.e. spatial multiplexing), and larger allowable operation bandwidths. The next two sections will outline two application cases of such mm-wave RFIDs, for long-range sensing and Gbps communications.

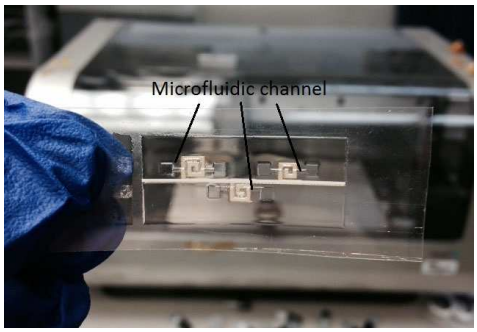

Fig. 5. An all-inkjet-printed microfluidics muti-sensing platform with an inkjet printer in the background [6].

B. Ultra-long-range low-cost printed sensing targets

1) Chipless: Chipless tags such as the one shown in Fig. 1 can be enabled with sensing capabilities, insofar as their scattering properties can be influenced by their environment. Considerations about the magnitude and the nature of such changes are critical for such devices. Indeed, small RCS magnitude changes, compounded with the detection challenges described in Sec. II-A1, can limit the reading ranges to a few cm, unless higher performance interrogation approaches are utilized [2]. Shifts in resonant frequencies, on the other hand, are generally much more detectable, an effect that was utilized in the tag of Fig. 1 by taking advantage of the humidity-dependent dielectric permittivity of the Kapton HN substrate that it is printed on. The measured shift of its resonant frequency, as a function of relative humidity level, along with its modeled counterpart can be seen in Fig. 4

Sensing and encoding in Chipless RFIDs can also be implemented by using printed microfluidic-channel-embedded resonators [7], [8]. A three microfluidics sensor chipless RFID platform is shown in Fig. 5 [6]. Although the three sensors are integrated on the same platform, they can still operate independently as shown in Fig. 6: while the sensor 2 is filled with different concentration glycerol water mixture and the other two sensors remain empty, the sensor 2 resonant frequency shift with liquid inside and the other two resonant frequencies are very stable.

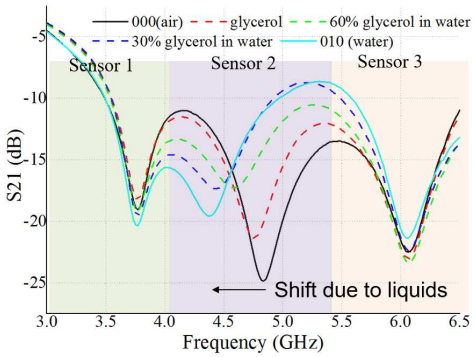

Fig. 6. Measured S21 values of the muti-sensing platform in Fig. 5 [6].

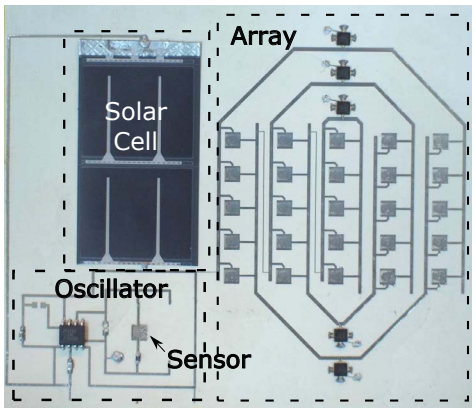

Fig. 7. Inkjet-printed Van-Atta backscatter reflectarray sensing node [9]

2) Long-range 5G IoT backscatter node: Work presented in [9] reported the first implementation of a mm-wave backscatter sensing RFID. The tag, shown in Fig. 7, integrates a 28 GHz reflectarray printed onto a flexible LCP substrate with single-transistor switches used to modulate its RCS, an inkjet-printed carbon-nanotubes-based ammonia sensor, a flexible amorphous-silicon solar cell, and a low-power timer to apply a modulation signal onto the switches.

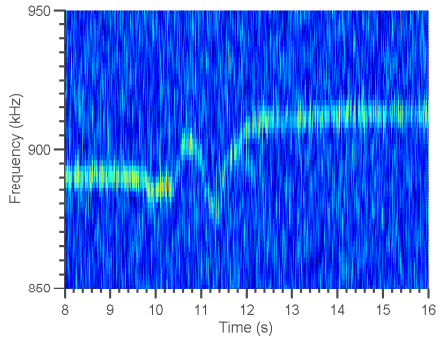

Fig. 8. Wirelessly measured real-time spectrogram of the modulation frequency applied by the timer of the device of Fig. 7, during an ammonia sensing event [9]

In this system, the modulation frequency applied by the

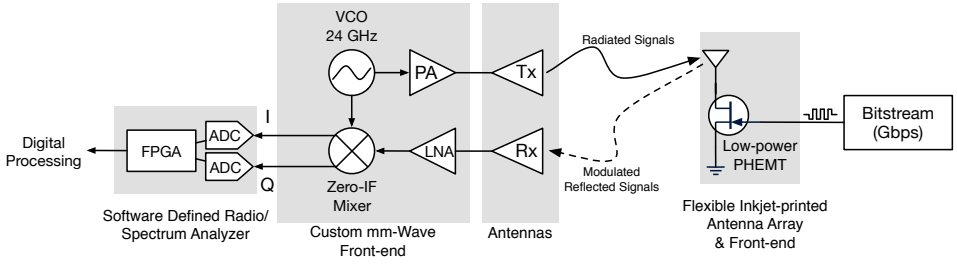

Fig. 9. End-to-end millimeter-wave backscatter system for Gigabit/second communication [10].

timer depends on the value of the resistance of the printed resistometric gas sensor. Exposure to ammonia changes the resistivity of the sensor which, consequently, changes the modulation frequency of the RCS. For demonstration purposes, this tag was exposed to ammonia and illuminated with a $28\,\mathrm{GHz}$ CW from the reader, with which the response was mixed for downconversion. The output of this process can be seen in Fig. 8. This work also demonstrated the longest reading range for a backscatter tag with a demonstrated reading range in excess of $80\,\mathrm{m}$ [9], with current effort geared towards extending it to $1\,\mathrm{km}$.

C. Low-cost short-range Gbps backscatter nodes

The first-ever reported Gbps backscatter transmission was recently demonstrated at millimeter-wave frequencies, dramatically expanding the potential of backscatter radio as a low-energy, low-complexity communication platform [10]. An end-to-end mmWave backscatter system for communication and sensing operating in the 24–28 GHz band was designed. In this band, miniaturized high-gain antennas and antenna arrays can be implemented, in contrast to UHF bands, where antenna arrays can become bulky and impractical. The miniaturization that is possible in mmWave bands allows for system implementation with additive manufacturing technologies (AMTs) and direct integration with wearable and flexible electronics for mobile health, sensing, security, and short-range ultra high-speed data transmission. To achieve broadband data transmission, the backscattering operation is leveraged to reflect subcarrier signals of GHz-level frequencies, which enables multi-gigabit communication with single transistor front-ends and pJ/bit energy consumption.

The mmWave backscatter system consists of a communicator and a custom reader front-end (Fig. 9). The backscatter communicator/tag consists of a common-source low-power enhancement P-HEMT transistor that is directly interfaced to a 5×1 antenna array through its drain (Fig. 10) while its gate is biased with a positive voltage. The voltage pulses applied to the gate modulate the transistor's channel width and modify the system's reflection coefficient.

The custom reader front-end consists of a voltage-controlled oscillator that generates a 24-GHz continuous wave (CW) passing through a power amplifier (PA) and radiated through a linearly-polarized transmit (Tx) horn antenna. The receive chain of the measurement setup consists of a receive (Rx) antenna that is cross-polarized with respect to the Tx antenna to a) achieve high Tx/Rx isolation and b) reject structural scattering from the backscatter tag's ground plane. The received signals are amplified with a low-noise amplifier (LNA) stage and are directly down-converted to DC with a zero-intermediate frequency (IF) mixer. The baseband in-phase (I) and quadrature (Q) signals are routed to the inputs of a digital oscilloscope or of a software-defined radio (SDR) for digital processing and demodulation.

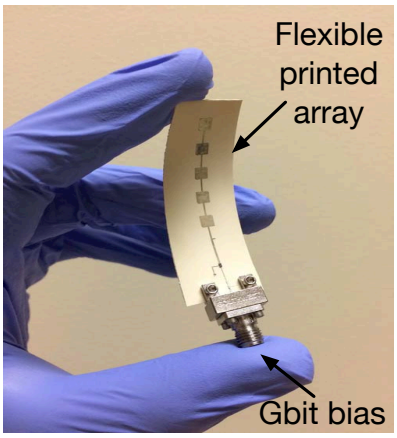

Fig. 10. Inkjet-printed 5×1 antenna array target with Gbit/second modulator [10].

The full potential of the implemented front-end is tested by biasing the tag with ultra high frequency subcarriers up to 5 GHz, in sharp contrast with the kHz–MHz-range subcarriers that are commonly used for backscatter tags in the UHF bands. Multiple tests have been conducted with frequency biasing from 500 MHz to 5 GHz. The received subcarriers around the frequencies of 2 GHz and 4 GHz can be clearly seen in Fig. 11, being 20–30 dB above the noise floor. A signal-to-noise ratio (SNR) estimate of the maximum versus the average channel power can be seen in Fig. 11-bottom, where it is apparent that a high-SNR, wideband operation can be achieved up to 4 GHz. This graph includes the *complete, compound* response of the *end-to-end system*, including the bandwidth of the front-end's magnitude difference between its two modulation states reflection coefficients ($|\Delta\Gamma|$), the printed antenna array's bandwidth, Tx chain VCO and PA efficiency, as well as Rx chain LNA and mixer bandwidth.The system shows an

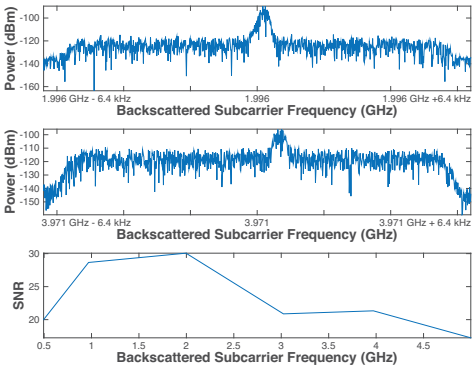

Fig. 11. Backscattered subcarrier at 2 GHz and 4 GHz, and SNR versus subcarrier frequency [10].

achievable end-to-end bandwidth of at least 4 GHz, which can enable extremely high data rates, considering the low complexity of the backscatter modulator/target.

Most importantly, at the subcarrier frequencies of 4 GHz and maximum biasing of 1 V, the front-end's static and dynamic (switching) power consumption are 200 nW and 0.6 mW, respectively, reaching an ultra-low energy-per-bit of less than $E_b = 0.15$ pJ/bit at 4 Gbps binary modulation (transistor on/off). Because of the high and flat frequency response from 1 to 2 GHz, high-order constellations can be used with reduced bandwidth occupancy (QPSK/16-QAM) which results in multi-gigabit transmission rates at increased energy efficiency levels, leveraging the backscatter operation to 5G-level datarates.

III. Towards Additive-Manufacturing-Enabled Low Cost Packaging and Integrated Radar Modules

To enable widespread incorporation of smart functionality into existing environments and consumer products for the IoT, low-cost scalable methods for the integration of mm-Wave semiconductors and interconnects are vital towards achieving low cost, ubiquitous devices. Traditionally, circuit design focuses around a planar substrate which carries most relevant circuitry and dies, meticulously organized to reduce size, while considering compact interconnects between layers, and layout for properly design transmission lines. On the die level, there are significant considerations for the matching of the coefficient of thermal expansion (CTE) between components and substrates to reduce delamination and other mechanical failures. Additionally, most current methods of microelectronic packaging involve wire bonding which introduces mismatch losses, often due to high parasitic inductance. Next generation IoT devices require minimal losses and optimal performance on virtually any substrate, although traditional approaches may become a limiting factor.

1) Additive manufacturing for high-performance mmW interconnects and packaging: Recent advancements in additive manufacturing (AM) has enabled its utilization to integrate multiple components into microelectronic packages for more compact, higher performing wireless systems. These fabrication technologies utilize a wide range of materials in a complex manner through scalable and cost efficient means by reducing material waste and tooling costs. The additive deposition of materials enables the integration of circuitry onto virtually any solid substrate, which is crucial for integration of multichip modules (MCM) and systems on modern substrates such as flexible or biodegradable low cost organics. This also applies to the incorporation of mm-Wave radar systems onto substrates that may be already available within a product, which can remove the requirement for a dedicated circuit board entirely depending on the design. The integration of printed passives into the package enables a potential reduction in device size, where additive methods enable the printing of exotic materials in picoliter volumes for high performance components, such as ferromagnetic nanoparticles to realize high performance inkjet-printed inductors [11]. With the ability to fabricate devices in a rapid roll-to-roll fashion while maintaining a high resolution, scalable, stretchable and rollable designs can be achieved enabling low cost, light weight antenna arrays for complex reconfigurable radar systems.

The properties enabling the deposition onto a wide range of substrates also enables the "on-demand" deposition of conductors (using silver nanoparticle inks) and dielectrics (using polymer-based inks) directly onto wireless integrated circuit (IC) dies, which can then be utilized for low loss interconnects, as seen in Fig. 12, where printed coplanar waveguide (CPW) transmission lines are directly integrated to create 3D ramped interconnects for mm-Wave dies as an alternative to traditional wire bonding [12]. With the ability to deposit printed layers as thin as 500 nm, additive technologies enable thin and flexible-compatible packaging while maintaining the hermetic properties necessary for next generation low cost, high performance requirements of mm-Wave and 5G IoT designs. Interconnects from dies with minimal distances to external components, such as on-package antennas, passives, and phase delay features have the potential to improve the overall performance of the wireless/radar system compared to traditional packaging methods.

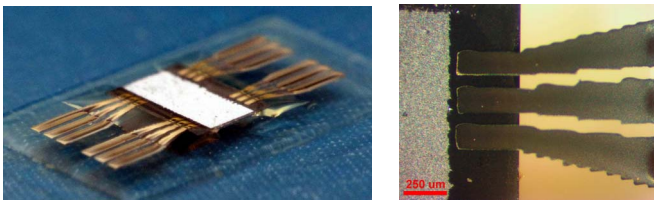

(a) (b)

Fig. 12. Inkjet-printed 3D coplanar waveguide (CPW) interconnects for printed mm-Wave system-in-package (SiP) design schemes: (a) perspective image, (b) detail micrograph [12].

2) 3D printing for compact IoT modules: 3D printing further enables low-loss compact package designs utilizing 3D multi-plane stacking to reduce the necessary surface area to fabricate designs for radar applications. The stacking of circuit topologies and components enables further reductions in the

distance between actives, passives, or a combination of these devices, minimizing interconnection losses and increasing system-level efficiency. The method of stereolithography 3D printing uses a DLP-based light source to cure thin layers of a photopolymer resin to build up 3D features. The maskless exposure system enables scalability that exposes and cross-links an entire layer simultaneously, in contrast to laser-based systems requiring rasterization. Along with inkjet printing for multilayer metallization purposes, the two technologies in combination offer a practical method of creating intelligent application-specific packages for wireless/radar systems, thus enabling the integration of heterogeneous features directly within a single wireless package, such as dielectric lenses, 3D transmission line interconnects, passives, and antenna arrays, as seen in Fig. 13 highlighting several printed demonstrations [13]. This method of fully printed 3D system-in-package (SiP) integration further reduces interconnect losses and system size, enabling high density radar systems with reduced surface area for miniaturized IoT devices, utilizing fewer tooling processes and highlighting a wider range of system-level configurations. With the appropriate additive toolset, full systems including batteries, antenna arrays, microfluidic channels for biomedical applications, and more have the possibility to be integrated into a single fully 3D package that offers low cost and high performance.

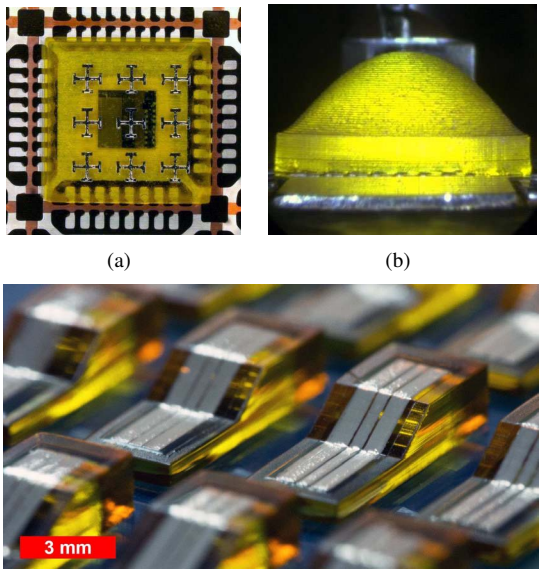

(a) (b)

(c)

Fig. 13. 3D/inkjet-printed intelligent packaging: (a) wireless shielding on a metallic $5\,\mathrm{mm} \times 5\,\mathrm{mm}$ quad flat no-lead (QFN) leadframe, (b) dielectric lens integration with a metallic $5\,\mathrm{mm} \times 5\,\mathrm{mm}$ QFN leadframe, (c) sloped through-mold via (TMV) transmission line interconnects [13].

IV. Conclusion

The printed devices presented in this work exhibit a remarkable, unique, and powerful combination of properties for their use as batteryless smart skin sensing nodes for the IoT. Their operation is made possible by the use of radar readers whose cost has been plummeting within the last decade, and will continue to do so thanks to the low-cost and high-performance of the packaging solutions enabled by the additive manufacturing revolution. Nevertheless, much progress can still be achieved in research pertaining to radar-reader/tag optimal architectures, interrogation schemes, data processing and channel modeling. This exciting, valuable, and emerging application area for radar technologies is now opening a large landscape of new opportunities for high-impact applicability to enhanced range (1km+) IoT and smart sensing systems.

V. Acknowledgment

The authors would like to acknowledge the support of DTRA, NSF and Lockheed Martin for this work.

References

[1] J. G. D. Hester and M. M. Tentzeris, "Inkjet-printed flexible mm-wave Van-Atta reflectarrays: A solution for ultra-long-range dense multi-tag and multi-sensing chipless RFID implementations for IoT Smart Skins," *IEEE Trans. Microw. Theory Tech.*, vol. 57, no. 5, pp. 1303–1309, May 2017.

[2] D. Girbau, A. Ramos, A. Lazaro, S. Rima, and R. Villarino, "Passive wireless temperature sensor based on time-coded UWB chipless RFID tags," *Microwave Theory and Techniques, IEEE Transactions on*, vol. 60, no. 11, pp. 3623–3632, Nov 2012.

[3] J. G. Hester and M. M. Tentzeris, "Inkjet-printed van-atta reflectarray sensors: A new paradigm for long-range chipless low cost ubiquitous smart skin sensors of the internet of things," in *2016 IEEE MTT-S International Microwave Symposium*. IEEE, 2016, pp. 1–4.

[4] D. Henry, J. Hester, H. Aubert, P. Pons, and M. Tentzeris, "Long range wireless interrogation of passive humidity sensors using van-atta cross-polarization effect and 3d beam scanning analysis," in *International Microwawe Symposium (IMS)*, 2017, p. 4p.

[5] V. Palazzi, J. Hester, J. Bito, F. Alimenti, C. Kalialakis, A. Collado, P. Mezzanotte, A. Georgiadis, L. Roselli, and M. M. Tentzeris, "A novel ultra-lightweight multiband rectenna on paper for rf energy harvesting in the next generation lte bands," *IEEE Transactions on Microwave Theory and Techniques*, 2017.

[6] W. Su, Q. Liu, B. Cook, and M. Tentzeris, "All-inkjet-printed microfluidics-based encodable flexible chipless rfid sensors," in *2016 IEEE MTT-S International Microwave Symposium (IMS)*, May 2016, pp. 1–4.

[7] S. Preradovic, I. Balbin, N. C. Karmakar, and G. F. Swiegers, "Multiresonator-based chipless rfid system for low-cost item tracking," *IEEE Transactions on Microwave Theory and Techniques*, vol. 57, no. 5, pp. 1411–1419, 2009.

[8] W. Su, J. Cooper, B. Cook, M. Tentzeris, C. Mariotti, and L. Roselli, "Inkjet-printed dual microfluidic-based sensor integrated system," in *IEEE SENSORS*, 2015, pp. 1–3.

[9] J. G. D. Hester and M. M. Tentzeris, "A mm-wave ultra-long-range energy-autonomous printed rfid-enabled van-atta wireless sensor: At the crossroads of 5g and iot," in *2017 IEEE MTT-S International Microwave Symposium (IMS)*, June 2017, pp. 1557–1560.

[10] J. Kimionis, A. Georgiadis, and M. M. Tentzeris, "Millimeter-wave backscatter: A quantum leap for gigabit communication, RF sensing, and wearables," in *2017 IEEE MTT-S Int. Microw. Symp.*, jun 2017, pp. 812–815.

[11] H. Lee, B. S. Cook, K. P. Murali, M. Raj, and M. M. Tentzeris, "Inkjet printed high-q rf inductors on paper substrate with ferromagnetic nano-material," *IEEE Microwave and Wireless Components Letters*, vol. 26, no. 6, pp. 419–421, June 2016.

[12] B. K. Tehrani, B. S. Cook, and M. M. Tentzeris, "Inkjet-printed 3d interconnects for millimeter-wave system-on-package solutions," in *2016 IEEE MTT-S International Microwave Symposium (IMS)*, May 2016, pp. 1–4.

[13] B. K. Tehrani, R. A. Bahr, W. Su, B. S. Cook, and M. M. Tentzeris, "E-band characterization of 3d-printed dielectrics for fully-printed millimeter-wave wireless system packaging," in *2017 IEEE MTT-S International Microwave Symposium (IMS)*, June 2017, pp. 1756–1759.